Hollow antiresonant fibers with reduced attenuation

Walter Belardi* and Jonathan C. Knight

Centre for Photonics and Photonic Materials, Department of Physics, University of Bath, Claverton Down, Bath BA2 7AY, UK
**Corresponding author: w.belardi@bath.ac.uk*

Received January 15, 2014; revised February 6, 2014; accepted February 21, 2014;
posted February 24, 2014 (Doc. ID 204841); published March 21, 2014

An improved design for hollow antiresonant fibers (HAFs) is presented. It consists of adding extra antiresonant glass elements within the air cladding region of an antiresonant hollow-core fiber. We use numerical simulations to compare fiber structures with and without the additional cladding elements in the near- and mid-IR regimes. We show that realizable fiber structures can provide greatly improved performance in terms of leakage and bending losses compared to previously reported antiresonant fibers. At mid-IR wavelengths, the adoption of this novel fiber design will lead to HAFs with reduced bending losses. In the near-IR, this design could lead to the fabrication of HAFs with very low attenuation.

OCIS codes: (060.2280) Fiber design and fabrication; (060.2400) Fiber properties; (060.4005) Microstructured fibers.
http://dx.doi.org/10.1364/OL.39.001853

Guidance of light in air has attracted attention since the dawn of optical fiber technology [1,2]. The field has made major advances since the discovery and development of photonic crystal fibers [3]. Hollow-core photonic bandgap fibers (HC-PBGFs) [4,5] proved to be able to guide light in air with attenuation as low as 1.2 dB/km at 1.62 μm wavelength [6]. Another type of hollow-core fiber known as "Kagomé" fiber [7] has also been developed for its particular characteristic of combining relatively low attenuation with broad bandwidth [8]. Although it does not possess a photonic bandgap cladding, it guides light with reduced leakage compared to a standard capillary because of the presence of an antiresonant glass layer [9,10] surrounding the air core.

It has been shown that the performance of Kagomé fibers is mainly due to the first silica layer around the air core [11,12]. The core modes do not decay exponentially in the cladding, and so increasing the cladding thickness has only a small impact on loss reduction. Leakage is instead limited by the rate of coupling into cladding modes. This understanding led to simplified designs for hollow antiresonant fibers (HAFs) comprising a single silica ring around a central air core [12]. Recently, it was shown [13–16] that adoption of a "negative curvature" core boundary (as shown in the HAF structure in Fig. 1) can lead to further loss reduction.

In this Letter we introduce a modified form of HAF (structure 1AE in Fig. 1) in which we reduce the coupling from the core into the cladding voids by introducing additional antiresonant elements into the voids. We show with numerical simulations that the level of leakage and bending loss of HAFs can be effectively and substantially reduced by the addition of such elements in realizable fiber structures.

We used Comsol to perform our numerical simulations. Figure 2 shows the transmission spectrum (between 2.75 and 3.8 μm) of the different fiber structures modeled.

The standard HAF modeled has the same core radius ($R_c = 47$ μm), silica wall thickness ($t = 2.66$ μm), and core boundary curvature ($\mathrm{Curv} = 2/d = 34322\ \mathrm{m}^{-1}$) as the fiber reported experimentally in [15] and that simulated in [16]. The cladding hole diameter in the HAF is $d = 58.27$ μm. In the modified design 1AE, we have inserted extra glass rings (with inner diameter d_1) nested within the original ones. While the silica thickness of these inclusions is still the same as in HAF (t), so that it is also antiresonant, the diameter d_1 is half of d. The third structure (2AE) is obtained in a similar way, and the diameter of its extra cladding rings is chosen to be $d_2 = d_1/2$.

We can compare the level of leakage loss of the different structures by looking at all the broken lines in Fig. 2.

The oscillations of the leakage losses at longer wavelengths are related to the coupling between the silica cladding modes and the fundamental-like core mode of the fiber. The origin of this resonant coupling has been described in Ref. [16]. Overall the leakage loss is reduced by several orders of magnitude by passing from the standard HAF design to the 2AE structure. Even in the case of 1AE, leakage losses are reduced below 0.1 dB/km.

In Fig. 2 we have also plotted the total calculated losses of the considered fiber structures when the material attenuation is taken into account (data from Ref. [17]). For all structures the fraction of power of the fundamental-like core mode in the silica is somewhat less than 10^{-4} [16]. Since silica attenuation at about a 3 μm wavelength is of the order of 100 dB/m [18], it becomes the main factor limiting fiber attenuation when

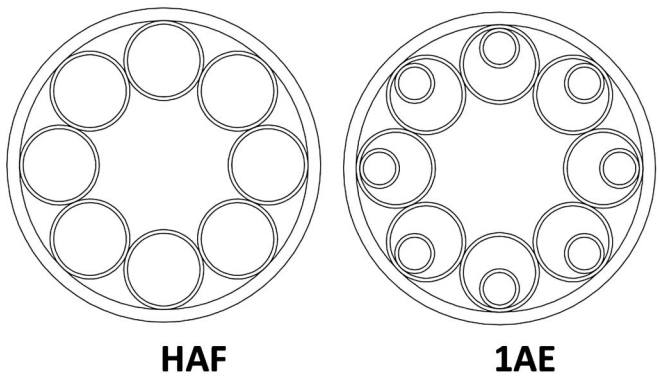

Fig. 1. HAF represents the current state of the art in hollow-core antiresonant fibers. Attenuation in the HAF is limited by coupling to the voids in the cladding. In the modified structure 1AE, this coupling is suppressed by including additional antiresonant elements within the cladding voids.

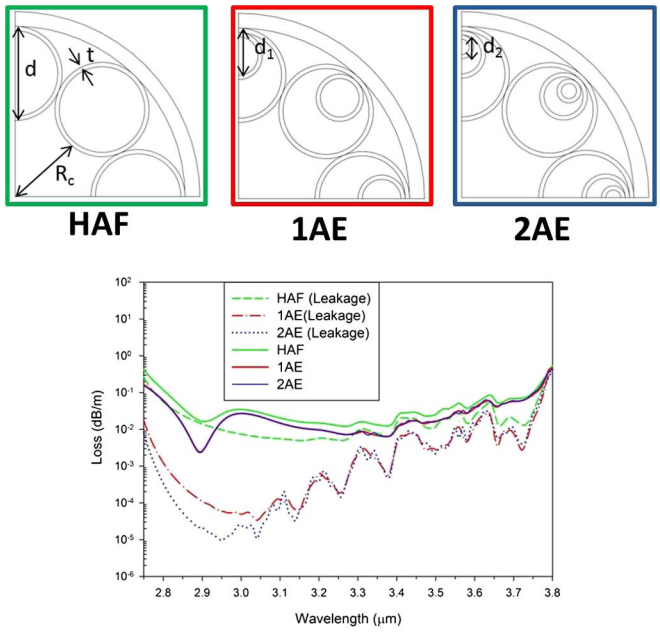

Fig. 2. Comparison between different fiber structures: current state-of-the-art hollow antiresonant fiber (HAF, green curve), one additional nested element (1AE, red curve), and two additional nested elements (2AE, blue curve). Note that the solid red and blue curves are coincident. The broken lines represent the leakage losses only while the solid lines include the effects of material attenuation of fused silica.

the leakage loss is reduced below about 0.01 dB/m. We can clearly see this effect by looking at the solid lines of Fig. 2. The level of loss for the HAF (solid green line), 1AE (solid red line), and 2AE (solid blue line) are almost the same (note also that the red and blue lines perfectly overlap).

We have investigated the fiber bending losses (computed as in [16]) to explore the effects of the proposed structural modifications on fiber performance.

The results, at a wavelength of 3.05 μm, are shown in Fig. 3. The solid lines show the total fiber loss, while the broken lines show the leakage loss for bend radii between 5 and 40 cm. In the case of the HAF structure (green line), we can notice the presence of local attenuation peaks [16] and an increase in the attenuation level when smaller bend radii are adopted. Figure 3 shows that in the case of the 1AE (red line) and 2AE (blue line) structures, the bending losses no longer exhibit the additional peaks and the total losses (solid lines) are dominated by the fiber material attenuation in this parameter range.

With silica as the fabrication material, the advantages of the structures with additional cladding elements can perhaps be better exploited at shorter wavelengths, where material attenuation is reduced. We have scaled down the structural dimension of the HAF, 1AE, and 2AE structures by a factor of 3 by replacing their geometrical parameters with the new values $t' = t/3$, $d' = d/3$, and $R_c' = R_c/3$. Figure 4 shows the transmission spectra for the scaled fiber structures between 0.95 and 1.4 μm.

In this wavelength range the attenuation of dry F300 silica is of the order of 10^{-3} dB/m [18] or less. Since in these fiber structures the fraction of optical power

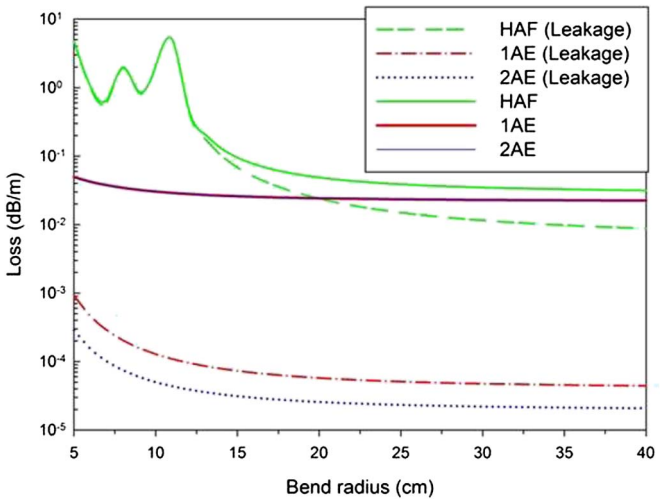

Fig. 3. Predicted losses of the HAF (green line), 1AE (red line), and 2AE (blue line) structures as a function of the fiber bend radius. The calculation of the leakage losses are represented with broken lines, while the loss calculations including silica attenuation are shown with solid lines. Note that the solid red and blue curves are coincident.

of the fundamental-like mode in the silica cladding is less than 10^{-4}, we can completely neglect the influence of the material attenuation on the total fiber losses.

Figure 4 shows a reduction of the leakage losses by over 2 orders of magnitude by adopting a 2AE structure (blue dotted line) as compared to the original HAF (green dashed line).

In this spectral range, the observed attenuation in HC-PBGFs is limited by surface scattering [6,19]. In the current design, the overlap of the guided light with the silica/air surfaces is far lower than in HC-PBGFs due in part to the larger core size. The ultimate limit to the attenuation attainable in these structures, therefore, is not currently known.

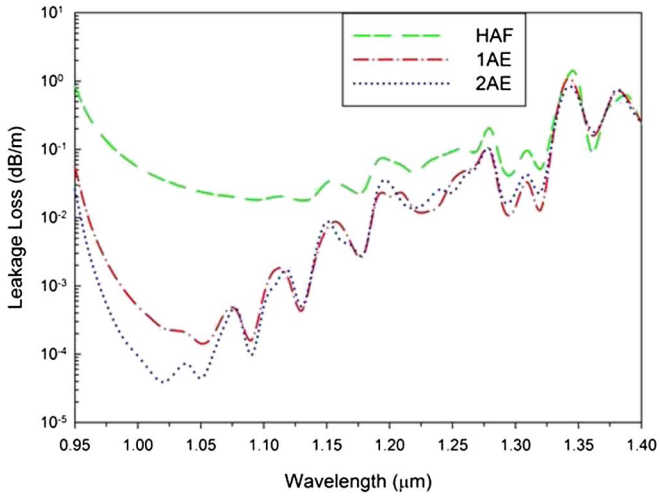

Fig. 4. Leakage loss between 0.95 and 1.4 μm for scaled HAF (green dashed line), 1AE (red dashed–dotted line), and 2AE (blue dotted line) structures. In this case the geometrical parameters for these three fiber structures have been modified to $t' = t/3$, $d' = d/3$, and $R_c' = R_c/3$.

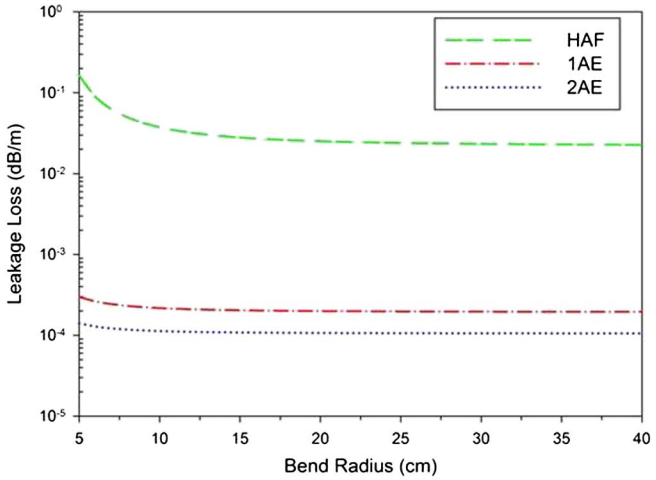

Fig. 5. Bending losses of the scaled HAF (green dashed line), 1AE (red dashed–dotted line), and 2AE (blue dotted line) structures. In this case the geometrical parameters for these three fiber structures have been modified to $t' = t/3$, $d' = d/3$, and $R_c' = R_c/3$.

Figure 5 shows the bending losses for the scaled structures, for a bend radius between 5 and 40 cm, at a wavelength of 1.06 μm.

As we can see, the leakage losses of the 1AE and 2AE structures are well below 1 dB/km and almost unaffected by bending for reasonable bend radii. With respect to the pure bending losses (i.e., the difference between the leakage losses at a certain bend radius and those of the "straight" fiber), we note that they are much lower for the scaled structure (Fig. 5) than in the case of the unscaled structure (Fig. 3), because we are studying a shorter wavelength but similar bend radii [20].

In order to illustrate the flexibility and feasibility of the proposed structures, we show in Fig. 6 the allowed tolerances for our design. We have considered the 1AE structure shown in the inset of Fig. 6, which has $t = 2.66$ μm, $d = 58.27$ μm, and $R_c = 47$ μm. Then we have calculated the leakage losses for this structure, at a wavelength of 3.05 μm, for different values of the internal hole diameter d_1 [Fig. 6(a)] and thickness t_1 [Fig. 6(b)].

As we can see from Fig. 6(a) ($t_1 = t$ in this case), the level of leakage losses is almost stable when the ratio of d_1 to d is kept between 0.4 and 0.6, and the leakage is well below 10^{-3} dB/m for any considered value of d_1. From Fig. 6(b) ($d_1 = d/2$ in this case), we can see that a large tolerance is also allowed for the thickness of the internal antiresonant element t_1 (±10%). We can calculate the optimum thickness $t_{1\mathrm{opt}}$ (corresponding to the minimum attenuation), just like in the case of the external thickness t, by using an antiresonant condition [9,10]:

$$t_{1\mathrm{opt}} = (2k+1)\frac{\lambda}{4\sqrt{n^2-1}} \qquad k = 0, 1, 2, \ldots, \qquad (1)$$

where k is an integer, $\lambda = 3.05$ μm is the operating wavelength, and $n = 1.418$ is the silica refractive index. We note that if the additional element is actually resonant (rather than antiresonant), then the attenuation is increased compared to the case of a standard HAF (dashed green line in Fig. 2), as one might expect. By working with low values of k, we therefore minimize the effect of variations in thickness. The observed tolerances lead us to conclude that the fiber performance will prove robust against realistic variations both in cross-section and along the length.

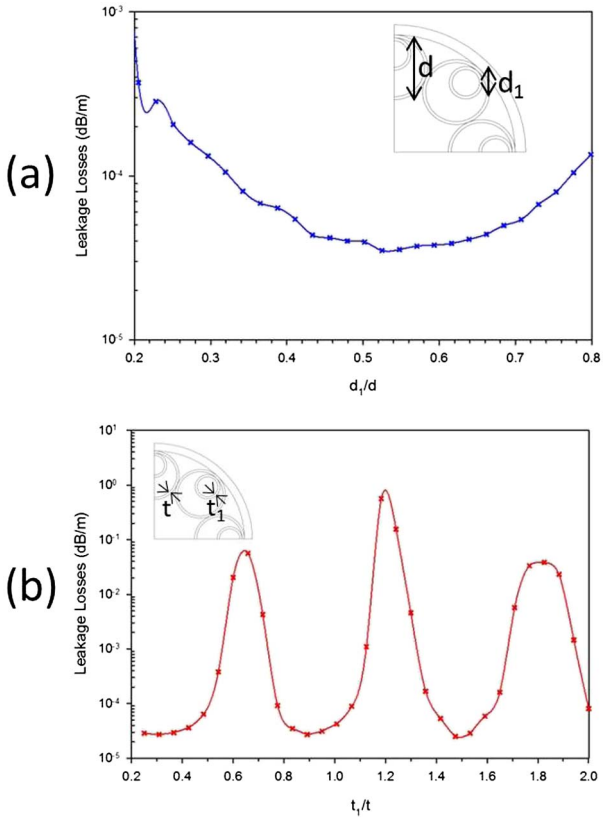

Fig. 6. Design tolerances for a 1AE structure at 3.05 μm ($t = 2.66$ μm, $d = 58.27$ μm, $R_c = 47$ μm). The leakage losses have been plotted (a) as a function of the internal cladding hole diameter d_1 and (b) as a function of the additional element thickness t_1.

In conclusion, we have presented a novel (to our knowledge) design for HAFs based on the insertion of additional antiresonant elements into the cladding holes. This realistic design modification substantially reduces leakage loss. It should allow the fabrication of HAFs with negligible leakage losses. At mid-IR wavelengths, where attenuation of existing silica-based HAFs is limited by material absorption, this will enable HAFs with low bending losses. At near-IR wavelengths, where silica attenuation is negligible, the proposed design should enable HAFs with very low attenuation. The large core size compared to low-loss HC-PBGFs may reduce the impact of scattering on the overall attenuation and make this fiber design competitive with HC-PBGFs with regard to attenuation.

This work was funded by the UK Engineering and Physical Sciences Council under EP/I011315/1.

References

1. E. Marcatili and R. Schmeltzer, Bell Syst. Tech. J. **43**, 1783 (1964).

2. P. Yeh, A. Yariv, and E. Marom, J. Opt. Soc. Am. **68**, 1196 (1978).
3. J. C. Knight, T. A. Birks, P. St. J. Russell, and D. M. Atkin, Opt. Lett. **21**, 1547 (1996).
4. J. C. Knight, J. Broeng, T. A. Birks, and P. St. J. Russell, Science **282**, 1476 (1998).
5. R. F. Cregan, B. J. Mangan, J. C. Knight, T. A. Birks, and P. St. J. Russell, Science **285**, 1537 (1999).
6. P. J. Roberts, F. Couny, H. Sabert, B. J. Mangan, D. P. Williams, L. Farr, M. W. Mason, A. Tomlinson, T. A. Birks, J. C. Knight, and P. St. J. Russell, Opt. Express **13**, 236 (2005).
7. F. Benabid, J. C. Knight, G. Antonopoulos, and P. St. J. Russell, Science **298**, 399 (2002).
8. F. Benabid, P. J. Roberts, F. Couny, and P. S. Light, J. Eur. Opt. Soc. **4**, 09004 (2009).
9. M. A. Duguay, Y. Kokubun, T. L. Koch, and L. Pfeiffer, Appl. Phys. Lett. **49**, 13 (1986).
10. J. L. Archambault, R. J. Black, S. Lacroix, and J. Bures, J. Lightwave Technol. **11**, 416 (1993).
11. G. J. Pearce, G. S. Wiederhecker, C. G. Poulton, S. Burger, and P. St. J. Russell, Opt. Express **15**, 12680 (2007).
12. S. Février, B. Beaudou, and P. Viale, Opt. Express **18**, 5142 (2010).
13. Y. Y. Wang, N. V. Wheeler, F. Couny, P. J. Roberts, and F. Benabid, Opt. Lett. **36**, 669 (2011).
14. A. D. Pryamikov, A. S. Biriukov, A. F. Kosolapov, V. G. Plotnichenko, S. L. Semjonov, and E. M. Dianov, Opt. Express **19**, 1441 (2011).
15. F. Yu, W. J. Wadsworth, and J. C. Knight, Opt. Express **20**, 11153 (2012).
16. W. Belardi and J. C. Knight, Opt. Express **21**, 21912 (2013).
17. G. Calingaert, S. Heron, and R. Stair, SAE J. **39**, 448 (1936).
18. O. Humbach, H. Fabian, U. Grzesik, U. Haken, and W. Heitmann, J. Non-Cryst. Solids **203**, 19 (1996).
19. P. J. Roberts, D. P. Williams, B. J. Mangan, H. Sabert, F. Couny, W. J. Wadsworth, T. A. Birks, J. C. Knight, and P. St. J. Russell, Opt. Express **13**, 8277 (2005).
20. W. A. Gambling, H. Matsumura, and C. M. Ragdale, Opt. Quantum Electron. **11**, 43 (1979).